Functionally Graded Segment of an Epitrochoidal Shells Structures– the Geometric Nonlinear Stress-Strain Analysis

Gil-Oulbé Mathieu, Svetlana L. Shambina, Dau Tyekolo, Ismel Taha Farhan

Abstract*: *The geometric nonlinear stress-strain state of functionally graded Epitrochoidal Shells under pressure and thermal environment is investigat-ed in this work. Material properties are taken as temperature dependent. Finite element solutions are obtained using the commercially soft-ware ANSYS. The effect of different geometry and material property parameters on the stress-strain state of functionally graded Epitro-choidal Shells under pressure and thermal environment is demonstrated. Finally, the change of the stresses, displacements, rotations and stains were investigated and presented.

Index Terms*: *Functionally Graded Material, Cyclic Shells, Functionally Graded Epitrochoidal Shell, Mechanical and Thermal Material Properties, Conserva-Tive, Non-Conservative, Block Lanczos Method, Spectral Transformations.

I. INTRODUCTION

The Madrid International Conference on Shells and Spatial Structure (ICSS) in 1989 gave rise to word wide more interest of architects for shells of complex geometry. Some of them are epitrochoidal shells which are investigat-ed in this article.

The generation of epitrochoidal surfaces

Let's take a point M in the plane of a circle of a radius a, rolling without sliding along another stationary circle with radius b, plots an epitrochoidal curve. The constant angle formed by these two circles is denoted by γ. The distance from a point M to the centre of the mobile circle is equal to μa (μ≥0).

The variation the angle γ from *0* to 2π generates a set of epitrochoidal curves that form epitrochoidal surfaces, which are middle surfaces of thin-walled epitrochoidal shells. According to the theorem of Joachimsthal, we may say that a family of the circles of an epitrochoidal surface is a family of the lines of principle curvatures, so the concerned surface is a special case of a canal surface of Joachimsthal.

An epitrochoidal surface (Figure 1) can be defined in an implicit form of definition as follows:

$$(x^2+y^2+z^2-2\mu a)^2=4a^2(x^2+y^2)$$

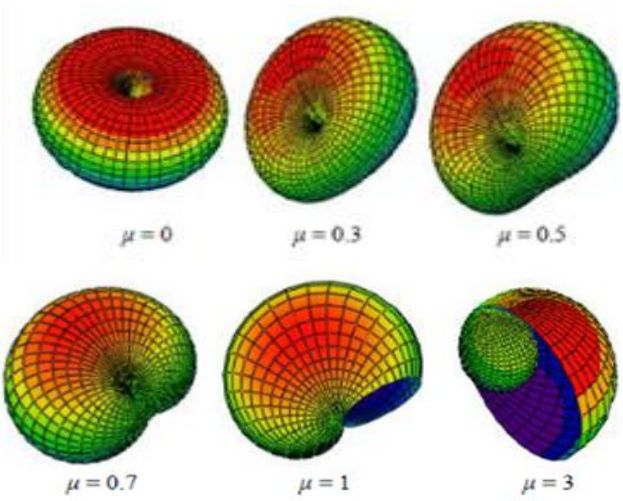

Figure 1. Epitrochoidal Surfaces

This implicit form of definition of an epitrochoidal surface has been described in [1], [2] for $a = b$. The plane *XOY* crosses an epitrochoidal surface along an epitrochoidal curve, which is called a "limaçon of Pascal" as well.

Parametrical equations are as follows:

$$x = x(\alpha,\beta) = 2R(\alpha)\cos^2(\beta)\cos(\alpha)$$

$$y = y(\alpha,\beta) = 2R(\alpha)\cos^2(\beta)\sin(\alpha)$$

$$z = z(\alpha,\beta) = R(\alpha)\sin(2\beta)\ ,$$

where $R(\alpha) = a(1+\mu\cos(\alpha))$. Here $R(\alpha)$ is the radius of a generatrix circle; α is the angle of the axis *Ox* with a plane of the generatrix circle$(0 \le \alpha \le 2\pi)$; $\beta = \frac{\gamma}{2}$ is an angle of the radius vector of the surface with the plane of the stationary circle $(-\frac{\pi}{2} \le \beta \le \frac{\pi}{2})$. Using this method of definition of a surface, one must remember that the surface is generated by rotation of a mobile circle with a radius a about its tangent at the point of tangency with the stationary circle of a radius $a = b$. Generatrix circles of the surface lie in the planes of one pencil.

Revised Manuscript Received on December 30,2018.

(co-first author). **Svetlana L. Shambina**, Peoples' Friendship University of Russia (RUDN University), 6 Miklukho-Maklaya Street, Moscow, 117198, Russian Federation,

Gil-Oulbé Mathieu, Peoples' Friendship University of Russia (RUDN University), 6 Miklukho-Maklaya Street, Moscow, 117198, Russian Federation,

Dau Tyekolo, Peoples' Friendship University of Russia (RUDN University), 6 Miklukho-Maklaya Street, Moscow, 117198, Russian Federation,

Ismel Taha Farhan, Peoples' Friendship University of Russia (RUDN University), 6 Miklukho-Maklaya Street, Moscow, 117198, Russian Federation,

The origin of the coordinates is in the double conic point of an epitrochoidal surface.

The surface is defined in a non-orthogonal and non-conjugate system of curvilinear coordinates. The vector form of definition of the surface is in the lines of principle curvatures:

$$r = r(\alpha,\beta) = 2R(\alpha)[cos(\alpha)\cdot i + sin(\alpha)\cdot j + \\ +R(\alpha)f(\beta)\cdot k]/D(\alpha,\beta)$$

,

where

$$D(\alpha,\beta) = 1 + R^2(\alpha)f^2(\beta)/a^2,$$

here $f(\beta)$ is any twice differentiable function.

The linear stress-stain analysis of a segment of an epitrochoidal shell under self-weight is investigated in work [3]. More information about these surfaces can be found in works [3], [4] and [5].

Let's consider a segment of an epitrochoidal shell structure with fixed supports as shown in Figure 2. This shell segment is under pressure and thermal loading. The thickness of the shell ($h=1.0$ *cm*) includes two layers (Al_2O_3 *= 5mm, steel = 5mm).* The edges of the shell are fixed.

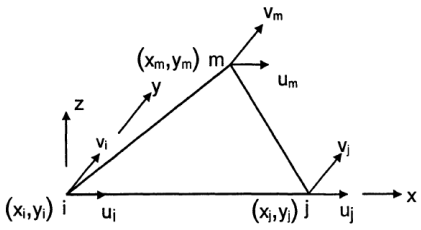

Figure 2: Triangular membra

The investigation of this segment is done in the geometric nonlinearity which in general represents the cases when the relations among kinematic quantities (i.e. displacement, rotation, and strains) are nonlinear. Such nonlinearities often occur when deformation is large.

Some papers [2], [6] are written concerning nonlinearity, and although there are many ways of categorizing different nonlinearities, it is generally accepted that four different sources of nonlinearity exist in solid mechanics.

Material nonlinearity represents the case when the relation between stress and strain is not linear.

Geometric nonlinearity, in general, represents the cases when the relations among kinematic quantities (i.e. displacement, rotation, and strains) are nonlinear.

Kinematic nonlinearity is also called boundary nonlinearity, depends on the deformations of the structure.

Force nonlinearity occurs when the applied forces depend on deformation.

1 Building material and method of analysis

The material of the shell is a functionally graded one, made of two layers of *ceramic* (Al_2O_3) and *metallic (steel).* This Functionally Graded Material (FGM, a composite material) is very resistant to high temperatures and high pressure. The mechanical and thermal material properties used in the present study are listed in Table 1.

Table 1. The mechanical and thermal material properties

Material	*Ceramic* (Al_2O_3)	*Metallic (Steel)*
Thermal expansion coefficient $\alpha(°c^{-1})$	$6.9x10^{-6}$	$14x10^{-6}$
Conductivity (k) (W/m°K)	*25*	*40*
Density $\left(\frac{kg}{m^2}\right)$	*3890*	*7850*
Jung's modulus, E(GPa)	*390*	*210*
Poisson's ratio	*0.25*	*0.25*

In this work, the Finite Element Method is used for modelling of functionally graded segment of an epitrochoidal shell with uniform thickness *h*.

Here, the derivation of the geometric stiffness matrix is somewhat different but consistent with the approach used throughout this text. The nonlinear equilibrium equations for a flat triangular shell element in its local coordinates system are first perturbed to yield the in-plane geometric stiffness matrix. Then out-of-plane considerations that involve the effect of rigid body rotations on member forces yield an out-of-plane geometric stiffness matrix. The shell element that was chosen for that purpose combines the constant stress triangle (CST), flat triangular membrane element and flat triangular plate element suggested in the discrete Kirchhoff theory (DKT).

4. Geometric Stiffness Matrix of Triangular Element Shells

The local geometric stiffness matrix of the shell element is split into three distinct matrices:

$$[K_G^e]_{TOTAL}^{shell} = [K_G^e]_{IP}^{mem} + [K_G^e]_{IP}^{plate} + [K_G^e]_{OP}^{shell}$$

where the first, second and third terms on the R.H.S. of the above equation represent the in-plane geometric stiffness matrix of the membrane, the in-plane geometric stiffness matrix of the plate and the out-of-plane geometric stiffness matrix of the shell element respectively.

The geometrically nonlinear triangular shell element has eighteen local degrees of freedom (DOF's): 3 displacements and 3 rotations at each node. The membrane element contributes to nine displacements DOF's only. The basic three nodded constant stress triangular flat element has only six local displacement DOF's that are shown in Figure 2. The out-of-plane contribution (the normal stiffness) of the membrane element to the basic local shell element is a displacement DOF in the direction which is normal to the plane of the element.

Finite element solution for the stress-strain behaviour of present FG model is proposed using Block Lanczos method in the software computation process.

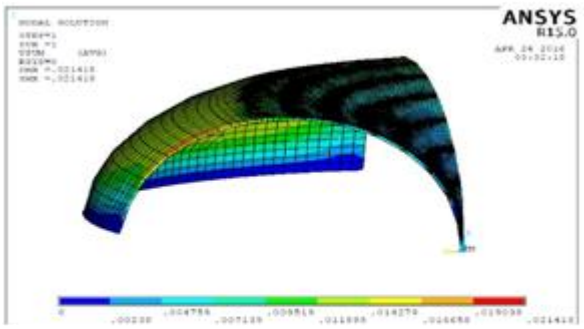

Figure 3. A displacement variation for FG segment of epitrochoidal shell

5. Block Lanczos method with spectral transformations

The Lanczos method [7], [8], [9] is recognized as a most powerful tool for extraction of large number of eigenpairs in large-scale problems of structural mechanics. The stability of its computational process is ensured by a selective or/and partial re-orthogonalization. For long Lanczos processes [10] the selective re-orthogonalization fails to succeed. On the contrary, the partial re-orthogonalization [9], [11] keeps Lanczos vectors highly orthogonal and ensures a highly stable computation. Therefore, we employ the block version of partial re-orthogonalization [12].

Conventional algorithms of Lanczos method possess the following disadvantage when the large-scale problems containing 60 000 - 500 000 and more equations are to be solved: at each step of Lanczos vector generation it is necessary to make the forward-back substitutions only for a single right-side vector *(r. s. v.)*. Due to this a lot of computation time is spent for input-output (*I/O*) operations because the upper part of the factored matrix U, where $K = LU$ and K is a stiffness matrix, must be read twice block-by-block from a secondary storage (disk) per each Lanczos vector.

The second problem is related to a drastic increase of amount of operations when the dimension of Krylov subspace (number of generated Lanczos vectors) is big enough (usually exceeds ~100). The block version of Lanczos algorithm is intended to reduce the *I/O* effort. Spectral transformations are implemented to split the long Lanczos process into a few relatively short ones. It reduces essentially the computation time when a large number of eigenpairs (100 - 1000 and more) are required.

The shell is modelled and analyzed with the commercial software ANSYS through its parametric design language (APDL) code. A shell element (SHELL181), defined in the ANSYS library, is used to discretize the FG segment of the epitrochoidal shell ($\mu=0.3$). This shell element has a total of six degrees of freedom per node i.e., translations and rotations, both in the x, y and z directions. The results of this numerical modelling are shown in Figures 3, 4, 5, 6, 7 and 8.

II. Results and Discussions

In this section, the stress-strain behaviour of FG segment of epitrochoidal shell is performed under pressure and uniform temperature field (T =700ºK). It is discretized and solved using finite element steps in ANSYS APDL platform.

Figure 3 shows displacement variation for FG segment of epitrochoidal shell under pressure and thermal loading. The overall displacement varies from 0.00m to 0.021418m.

Figure 4 shows the rotation variation for FG segment of epitrochoidal shell under pressure and thermal loading. The stress varies from 0.01557 to 0.140126.

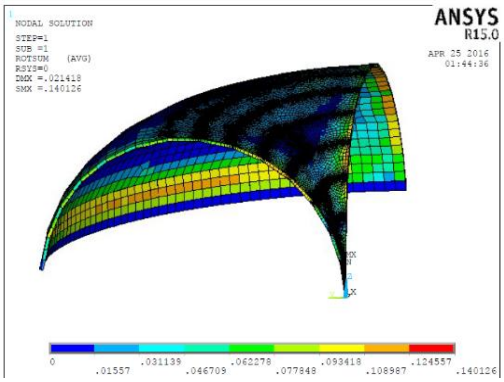

Figure 4. Rotation variation for FG segment of epitrochoidal shell

Figure 5 shows Von Misses total mechanical and thermal Strain variation for FG segment of epitrochoidal shell under pressure and thermal loading. The strain varies from -0.472·10-3 to 0.375822.

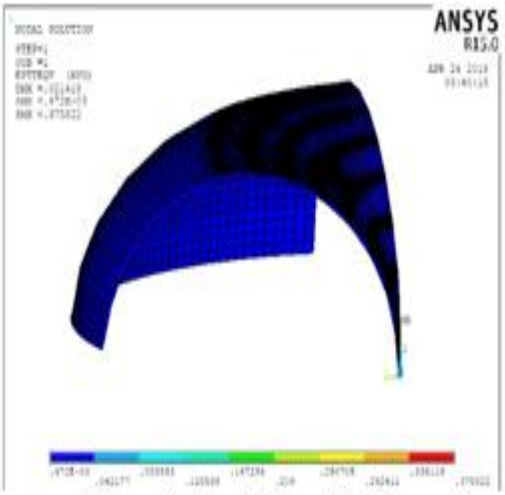

Figure 5. Von Mises of total mechanical and thermal strain variation for FG segment of epitrochoidal shell

Figure 6 shows X-component of total mechanical and thermal variation for FG segment of epitrochoidal shell under pressure and thermal loading. The strain varies from -0.3391 to 0.136443.

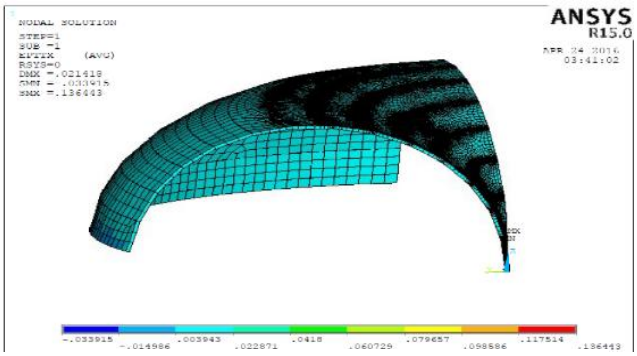

Figure 6. X-component total mechanical and thermal strain variation for FG segment of epitrochoidal shell

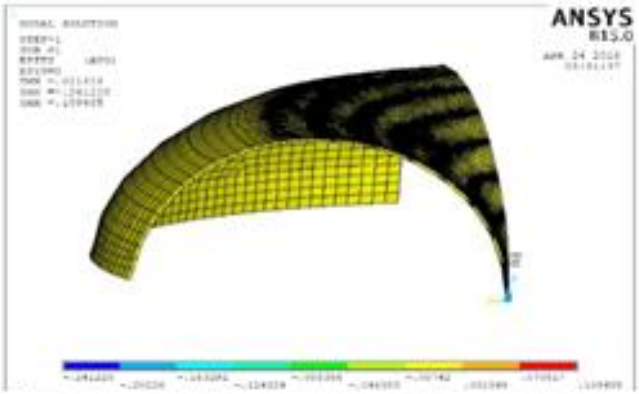

Figure 7: Y-component total mechanical and thermal strain variation for FG

Figure 7 shows Y-component of total mechanical and thermal variation for FG segment of epitrochoidal shell under pressure and thermal loading. The strain varies from -0.241228 to 0.109485.

III. CONCLUSIONS

In this study, the thermal stress-strain behaviour of FG segment of epitrochoidal shell under pressure and uniform temperature field are investigated. In addition, temperature dependent material properties of FGM constituents are considered. Finite element solution for the stress-strain behaviour of present FG model is proposed using Block Lanczos method. The influences of different material and geometrical parameters on the thermal stress-strain of FG segment of epitrochoidal shell are illustrated. Finally, the change of the stresses, displacements, rotations and stains were investigated and presented.

ACKNOWLEDGEMENT

This paper was financially supported by the Ministry of Education and Science of the Russian Federation on the program to improve the competitiveness of Peoples' Friendship University of Russia (RUDN University) among the world's leading research and educational centres in the 2016 – 2020.

REFERENCES

1. Mihailescu M., Horvath I., 1977. Velaroidal shells for covering universal industrial halls, Acta Techn. Acad. Sci. Hung.,85(1-2): 135-145.
2. Reddy, J.N., 2004. An Introduction to Nonlinear Finite Element Analysis, Publisher: Oxford University Press | ISBN: 019852529X | edition 2004 |Scan PDF |463 pages |101.9 mb.
3. Gil-oulbé Mathieu. The stress-strain ana ysis of epitrochoidal shells. – PhD thesis – Moscow – 1997.
4. Krivoshapko, S.N., Ivanov, V.N., 2015. Encyclopedia of Analytical Surfaces, DOI 10.1007/978-3-319-11773-7. Springer International Publishing Switzerland.
5. Krivoshapko, S.N., Mamieva, I.A., 2012. Outstanding space structures of the last 20 years, Journal Montazhn. i spetsial. raboti v stroitelstve, 12: 8-14.
6. Kim, Nam-Ho, 2015. Introduction to nonlinear finite element analysis, DOI 10.1007/978-1-4419-1746-1. Springer New York Heidelberg Dordrecht London © Springer Science+Business media New York.
7. Hughes, T.J.R., The finite element method, Prentice Hall, Englewood Cliffs, NJ, 1987
8. Parlett, B., The symmetric eigenvalue problem, Prentice-Hall, Englewood Cliffs, NJ, 1980.
9. Papadrakakis, M., Solving large –scale problems in mechanics, John Wiley & Sons Ltd., 1993.
10. Fialko, S.Yu., High-performance iterative and sparse direct solvers in Robot software for static and dynamic analysis of large-scale structures. Proceedings of the second European conference on computational mechanics, Poland, June 26- 29, 2001, 18 p.
11. Simon, H., The Lanczos algorithm with partial reorthogonalization, Math. Comp., 42, pp. 115-136, 1984.
12. Grimes, R.G. Lewis, J.G., Simon, H.D., A shifted block Lanczos algorithm for solving sparse symmetric generalized eigenproblems, SIAM J. Matrix Anal. Appl, V.15, 1: pp. 1- 45, 1994.